

# Circular RNA-AnnexinA7 accelerates cisplatin resistance in non-small cell lung cancer *via* modulating microRNA-545-3p to mediate Cyclin D1

Jian Yao✉, Hai Yang Zhang, Shuang Gu, Jin Long Zou, Qiang Zhang and Ri Chu Qu

Department of Thoracic Surgery, Jilin Provincial People's Hospital, Changchun City, Jilin Province, 130021, China

**Objective:** To explore the mechanism of circular RNA (circRNA)-AnnexinA7 (ANXA7) in non-small cell lung cancer (NSCLC) cisplatin (DDP) resistance through microRNA (miR)-545-3p to target Cyclin D1 (CCND1). **Methods:** DDP-resistant and non-resistant NSCLC tissues and normal tissues were collected. DDP-resistant cells (A549/DDP and H460/DDP) were constructed. circ-ANXA7, miR-545-3p, CCND1, P-Glycoprotein, and glutathione S-transferase- $\pi$  in tissues and cells were measured. Analysis of circ-ANXA7 ring structure was performed, as well as detection of circ-ANXA7 distribution in cells. Cell proliferation was detected by MTT and colony formation assay, apoptosis rate was detected by flow cytometry, and cell migration and invasion were evaluated by Transwell assay. The targeting relationship between circ-ANXA7, miR-545-3p and CCND1 was verified. Measurement of tumor volume and quality in mice was performed. **Results:** Circ-ANXA7 and CCND1 were elevated, while miR-545-3p was suppressed in DDP-resistant NSCLC tissues and cells. Circ-ANXA7 combined with miR-545-3p, which targeted CCND1 to expedite A549/DDP cell proliferation, migration, invasion, DDP resistance, but inhibited cell apoptosis. **Conclusion:** Circ-ANXA7 enhances DDP resistance in NSCLC *via* absorbing miR-545-3p to target CCND1 and might be a latent therapeutic target for NSCLC.

**Keywords:** Circular RNA-AnnexinA7, MicroRNA-545-3p, Cyclin D1, Target binding, A549/cisplatin cells

**Received:** 01 November, 2022; revised: 03 April, 2023; accepted: 11 April, 2023; available on-line: 23 May, 2023

✉e-mail: [yaojian@dmu-edu.cn](mailto:yaojian@dmu-edu.cn)

**Acknowledgements of Financial Support:** Science and technology development project of Jilin (No. 201903031605F).

**Abbreviations:** ANOVA, Analysis of variance; ANXA7, AnnexinA7; CCND1, Cyclin D1; circRNAs, Circular RNAs; DDP, Cisplatin; FBS, fetal bovine serum; FITC, Fluorescein isothiocyanate; GAPDH, Glyceraldehyde-3-phosphate dehydrogenase; GST- $\pi$ , Glutathione S-transferase  $\pi$ ; IgG, Immunoglobulin G; LC, Lung cancer; MTT, 3-(4,5-dimethylthiazol-2-yl)-2,5-diphenyltetrazolium bromide assay; MUT, Mutant type; NC, Negative control; NSCLC, Non-small cell lung cancer; P-gp, P-glycoprotein; PI, Propidium iodide; RIP, RNA immunoprecipitation; RT-qPCR, Reverse transcription quantitative polymerase chain reaction; S.D., Standard deviation; UTR, Untranslated region; WT, Wild-type

## INTRODUCTION

Lung cancer (LC) is a malignant tumor with the uppermost morbidity and mortality in the world (Zhang *et al.*, 2021). Non-small cell lung cancer (NSCLC) is an extremely critical type of LC, taking up about 85% of LC cases (Xu *et al.*, 2020). Treatment strategies for NSCLC have improved recently, but the 5-year survival rate is

still greatly reduced by about 10–15% (Xu *et al.*, 2021). Cisplatin (DDP) chemotherapy is a first-line anti-cancer chemotherapy agent in NSCLC. Nevertheless, patients treated with DDP for a long time develop DDP resistance (Wu *et al.*, 2020). As reported, around 63% of NSCLC patients have DDP resistance (Ye *et al.*, 2020). Consequently, lessening DDP resistance is the crux to ameliorating NSCLC patients' outcomes. This study was to comprehend latent mechanisms in NSCLC DDP resistance and identify latent biomarkers, offering brand-new insights into NSCLC therapy.

Circular RNAs (circRNAs), a non-coding RNA with closed continuous loops, have been testified to mediate primary or antitumor responses in different cancer treatments (Fan *et al.*, 2021). Notably, numerous circRNAs exert critical roles in multiple biological processes of NSCLC. For instance, circ\_PIP5K1A (Feng *et al.*, 2021), circ-RNF121 (Liu *et al.*, 2022) and circ\_0076305 (Wang *et al.*, 2021) have been reported to be implicated in the cancer progression and DDP resistance of NSCLC. Circ-AnnexinA7 (ANXA7), as a member of circRNA, has been reported to expedite lung adenocarcinoma progression (Wang, 2021). In the preliminary experiment, this circRNA was aberrantly modulated in DDP-resistant NSCLC tissues. Nevertheless, the latent impact of circ-ANXA7 on DDP resistance in NSCLC is unknown.

circRNA/miRNA/mRNA regulatory network has been adopted to elucidate circRNA's mechanism in multiple biological processes (Xu *et al.*, 2020). Bioinformatics predicted that miR-545-3p was the target of circ-ANXA7. Recently, miR-545-3p has been reported to participate in NSCLC progression. For instance, blocking circ\_0014130 restrains resistance and malignant behaviors of NSCLC cells *via* modulating miR-545-3p (Du *et al.*, 2021). Circ\_0072083 knockdown is involved in DPP-triggered NSCLC tumor inhibition through the miR-545-3p/CBLL1 axis (Li *et al.*, 2020). Nevertheless, it has not been reported that circ-ANXA7, as a competitive endogenous RNA, combined with miR-545-3p to participate in NSCLC DDP resistance.

Cyclin D1 (CCND1), a recognized cell cycle-associated protein, exerts a crucial action in cell cycle change (Meng *et al.*, 2021). CCND1 is a critical driver of malignant transformation and is frequently elevated in NSCLC, leading to the aberrant proliferation of NSCLC cells (Liu *et al.*, 2020). Notably, modulating CCND1 can alter DDP-resistant cell malignant phenotype (Ju *et al.*, 2020). In this study, it was hypothesized that circ-ANXA7 might participate in NSCLC DDP resistance *via* miR-545-3p to modulate CCND1.

In this study, 2 DDP-resistant NSCLC cell lines (A549/DDP and H460/DDP) were constructed, and

circ-ANXA7 was confirmed to modulate DDP-resistant NSCLC cell sensitivity and behavior. Additionally, this research further elucidated the action of circ-ANXA7/miR-545-3p/CCND1 axis in DDP resistance and cancerization of NSCLC.

## MATERIALS AND METHODS

### Clinical tissue specimen

90 tissue samples were obtained from the School of Medicine, University of Electronic Science and Technology of China, including 30 non-tumor tissue samples from patients with pulmonary laceration repair (control) and 60 NSCLC tissue samples from NSCLC patients with radical resection. Patients with progressive disease (PD) or postoperative recurrence less than 6 months were DDP-resistant, while patients without PD and postoperative recurrence over 12 months were non-resistant. All tissue samples were placed at  $-80^{\circ}\text{C}$ . Authorization of the study was performed by the Ethics Committee of the School of Medicine, University of Electronic Science and Technology of China, and written informed consent was obtained from all participants.

### Cell culture and transfection

NSCLC cell lines (A549 and H460) were purchased from American Tissue Culture Collection (Manassas, VA), and human bronchial epithelioid cells (HBE-1) were from Bena Culture Collection (Beijing, China). Cells were cultured in Roswell Park Memorial Institute-1640 medium (Hyclone, Logan, UT, USA) containing 10% fetal bovine serum, 100 U/ml penicillin and 100 mg/mL streptomycin (Gibco, Carlsbad, CA). DDP-resistant cells (A549/DDP and H460/DDP) were established and grown in a complete medium replenished with DDP (1  $\mu\text{g}/\text{mL}$ , Sigma-Aldrich, St. Louis, MO) to maintain resistance. All cells were cultured in 5%  $\text{CO}_2$  at  $37^{\circ}\text{C}$  (Pang *et al.*, 2020).

sh-circ-ANXA7, miR-545-3p mimic and inhibitor, as well as corresponding negative controls (sh-NC, mimic-NC, in-NC) were designed and generated (Ribo Biotech, Guangzhou, China). CCND1 overexpression plasmid was purchased from ORIGENE, with empty plasmid as NC. When cell confluence reached 70% to 80%, A549/DDP cells were plated into 6-well plates ( $1 \times 10^5$  cells/mL) and cultured for 24 h. Transfection of cells was performed using Lipofectamine 3000 (Invitrogen) (Hu *et al.*, 2021). Transfection concentrations of mimic and inhibitor were 50 nM and 20 nM, respectively, and 1  $\mu\text{g}$  and 2500 ng for sh-circANXA7 and CCND1 overexpressed plasmid, respectively. After 48 h, the transfection efficiency was evaluated by reverse transcription quantitative polymerase chain reaction (RT-qPCR) or Western blot.

### Ribonuclease R and actinomycin D assays

RNase R assay: total RNA (2  $\mu\text{g}$ ) from A549 cells was incubated with 3 U/ $\mu\text{g}$  RNase-R (07250, Epicentre Technologies, USA) at  $37^{\circ}\text{C}$  for 30 min. circ-ANXA7 and ANXA7 mRNA expressions were subsequently determined by RT-qPCR.

Actinomycin D test: Cells were cultured with or without 2  $\mu\text{g}/\text{mL}$  actinomycin D (Sigma, USA) and harvested at different points in time. Circ-ANXA7 and ANXA7 mRNA was determined by RT-qPCR (Wu *et al.*, 2020).

### Subcellular localization analysis

Cytoplasm RNA and nuclear RNA of cells were isolated using PARIS Kit (Invitrogen). Then, the examination of circ-ANXA7 in cytoplasm RNA and nuclear RNA was implemented by RT-qPCR. U6 and glyceraldehyde-3-phosphate dehydrogenase (GAPDH) were nuclear and cytoplasmic controls, respectively.

### RT-qPCR

Extraction of total RNA from NSCLC tissues and cells was done using Trizol reagent (Invitrogen). Reverse transcription of circRNA/mRNA and miRNA was performed with PrimeScript RT reagent Kit and miRNA First Strand Synthesis Kit (both Takara, Tokyo, Japan), respectively. RT-qPCR was performed with SYBR Green kit (Thermo Fisher Scientific, Waltham, MA, USA) and Mx3005P qPCR system (Agilent Technologies, Santa Clara, CA, USA). U6 and GAPDH were loading controls for miRNA and mRNA/circRNA, respectively. Primer sequences were presented in Table 1 (Song *et al.*, 2021).

### Western blot

Extraction of total protein was done with 500  $\mu\text{L}$  Radio-Immunoprecipitation assay lysis buffer (Beyotime, China). An equal amount of protein (20  $\mu\text{g}$ ) was separated by 8% sodium dodecyl sulfate-polyacrylamide gel electrophoresis (Solarbio), electroblotted onto polyvinylidene fluoride membranes (Invitrogen), and blocked with 5% skimmed milk, followed by incubation with primary antibodies CCND1 (ab134175, Abcam, 1:1000), anti-P-glycoprotein (P-gp) (ab170904, Abcam, 1:3,000), glutathione S-transferase  $\pi$  (GST- $\pi$ ) (ab233112, Abcam, 1:1,000) and GAPDH (1:7,500, ab8245) at  $4^{\circ}\text{C}$  overnight and horseradish peroxidase-conjugated goat anti-rabbit Immunoglobulin G (IgG) (1:1000, ab181236, Abcam) for 2 h. Visualization of the signal was performed with an enhanced chemiluminescence kit (34080, Thermo Fisher Scientific). Density analysis was performed with ImageJ software.

### 3-(4,5-dimethylthiazol-2-yl)-2,5-diphenyltetrazolium bromide (MTT) assay

A549/DDP cells ( $5 \times 10^3$ /well) were seeded into 96-well plates and cultured overnight. MTT reagent (beyotime) was added at different time points (0, 24, 48, 72 h) and incubated at  $37^{\circ}\text{C}$  for 4 h. Then, 150  $\mu\text{L}$  Dimethyl Sulfoxide was added to each well and 10 min later, optical density at 490 nm was read with a microplate reader (PerkinElmer) (Zhu *et al.*, 2021).

### Colony formation assay

A549/DDP cells ( $5 \times 10^3$ /well) were seeded in 12-well plates and cultured for 14 d, during which a fresh complete medium was replaced every 3 days and the wells were washed twice with PBS. Then, colonies were fixed in paraformaldehyde (4%, Beyotime), dyed with 0.1% crystal violet (Beyotime) for 2 h, and washed with  $\text{ddH}_2\text{O}_3$  times. The number of colonies was counted under an inverted microscope (Nikon).

### Flow cytometry

A549/DDP cells ( $1 \times 10^5$  cells/well) after DDP treatment were incubated for 48 h. Cell apoptosis was analyzed by Annexin V-fluorescein isothiocyanate (FITC)/Propidium iodide (PI) assay kit (BestBio, Shanghai, China). In brief, cells were rinsed with cold phosphate-

buffered saline (PBS) and incubated with 5  $\mu$ L Annexin V-FITC and 5  $\mu$ L PI for 20 min. Ultimately, the assessment of cell apoptosis was implemented on a flow cytometer (FACS Calibur flow cytometer) (Wei *et al.*, 2021).

### Transwell migration and invasion analysis

Transwell assay evaluated A549/DDP cell invasion and migration. For migration and invasion measurements, transwell chambers were used without or with Matrigel, respectively (Corning, USA). Cells were prepared at  $2 \times 10^6$  cells/mL, then 400  $\mu$ L cell suspension was inoculated into the upper chamber containing serum-free medium, and 10% FBS was added to the lower chamber. After 24 h of culture, cells in the upper layer were removed with cotton swabs, while those in the lower layer were fixed with methanol for 30 min, stained with 0.1% crystal violet, and counted in five fields under a microscope (Swiss taikang, magnification  $\times 100$ ) (Guo *et al.*, 2022).

### Luciferase activity assay

A549/DDP cells were plated on a 24-well plate. circ-ANXA7 or CCND1 3' untranslated region (UTR) (Promega) containing miR-545-3p wild-type (WT) or mutant-type (MUT) binding sites was inserted into the pmirGLO vector (Promega, Madison, WI), and circ-ANXA7/CCND1-WT 3'UTR and circ-ANXA7/CCND1-MUT 3'UTR reporter genes were named. Co-transfection of the corresponding luciferase reporter gene with miR-545-3p mimic or miR-NC was done in A549/DDP cells. After 48 h of incubation, the determination of the luciferase activity was implemented with the luciferase reporter gene kit (Promega) (Guo *et al.*, 2022).

### RNA immunoprecipitation (RIP) experiment

Anti-Ago2 (ab252812) and anti-IgG (ab109489) antibodies were utilized for detection. In short, cells were lysed with a lysis buffer and then incubated with protein-g magnetic beads-conjugated anti-Ago2 or IgG at 40°C for 6 h. Microbeads were later collected, and binding RNA was extracted to examine the enrichment of circ-ANXA7 and miR-545-3p (Zhang *et al.*, 2021).

**Table 1. Primer sequences**

Genes	Primer sequences (5'-3')
Circ-ANXA7	F: 5'-GCTATCCCCAACAGGCTAC-3'
	R: 5'-CCTGGTGGGACTCCAAATC-3'
MiR-545-3p	F: 5'-TGCCTCAGCAACATTTATTG-3'
	R: 5'-CCAGTGCAGGGTCCGAGGTATT-3'
CCND1	F: 5'-AGCTGTGCATCTACACCGAC-3'
	R: 5'-GAAATCGTGGGGTTCATTG-3'
U6	F: 5'-CTCGCTTCGGCAGCAC-3'
	R: 5'-AACGCTTCACGAATTTGCGT-3'
GAPDH	F: 5'-TCCATCACCATCTTCCA-3'
	R: 5'-CATCACGCCACAGTTTCC-3'

Note: F, forward; R, reverse.

### In vivo tumor growth test

The tumor formation experiment was conducted in BALB/c male nude mice (n=24, 6 weeks old, weight of 18–20 g, Huafukang, Beijing, China). A549/DDP cells transfected with sh-Circ-ANXA7, or sh-NC ( $1 \times 10^7$ ) were injected subcutaneously into the back of mice. Mice were divided into four groups: sh-NC+PBS, sh-NC+DDP, sh-circ-ANXA7+PBS, and sh-circ-ANXA7+DDP groups. DDP (5 mg/kg) or PBS was injected to measure the tumor volume once a week. After 4 weeks, transplanted tumors from euthanized mice were weighed. Animal treatments were approved by the Animal Research Committee of the School of Medicine, University of Electronic Science and Technology of China (Shao *et al.*, 2021).

### Statistical analysis

Statistical software SPSS 21.0 (SPSS, Inc, Chicago, IL, USA) was utilized to analyze data. Kolmogorov-Smirnov test checked the normal distribution of data, and the results were presented as mean  $\pm$  standard deviation (S.D.). Two-group comparisons were performed using t-test. Comparisons among multiple groups were imple-

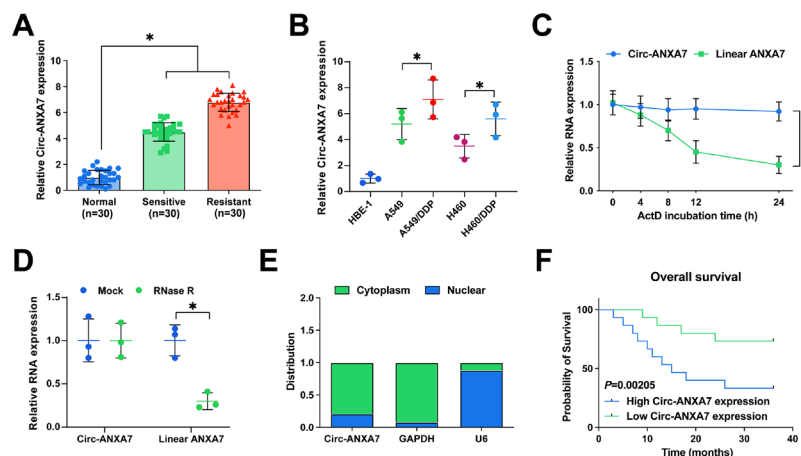


**Figure 1. Circ-ANXA7 is modulated in DDP-resistant NSCLC tissues and cells**

(A) RT-qPCR test of circ-ANXA7 in each tissue; (B) RT-qPCR examination of circ-ANXA7 in each cell; (C–D) RNase R and Actinomycin D determination of the stability of circ-ANXA7; (E) RT-qPCR test of the localization of circ-ANXA7 in A549/DDP cells; (F) Kaplan-Meier analysis of the survival prognosis of DDP-resistant NSCLC patients. Data were expressed as mean  $\pm$  S.D. (Number of samples = 3). \* $P < 0.05$ .

**Table 2. Clinicopathological characteristics of non-resistant and resistant patients**

Characteristic	Cases	Nonresistant cases (n=30)	Resistant cases (n=30)	P
<b>Age (year)</b>				
60 or less	33	17	16	0.859
More than 60	27	13	14	
<b>Gender</b>				
Male	35	19	16	0.554
Female	25	11	14	
<b>Circ-ANXA7 level</b>				
0.5 fold of control or less	27	19	8	<0.001***
More than 0.5 fold of control	33	11	22	
<b>Tumor size</b>				
Less than 5 cm	32	18	14	0.355
5 cm or more	28	12	16	
<b>Distant metastasis</b>				
No	34	18	16	0.438
Yes	26	12	14	
<b>Depth of invasion</b>				
N0/N1	26	18	8	0.041*
N2/N3	34	12	22	
<b>Differentiation</b>				
Good/Moderate	31	21	10	0.005**
Poor	29	9	20	

\* $P < 0.05$ . \*\* $P < 0.01$ . \*\*\* $P < 0.001$ .

mented with one-way analysis of variance (ANOVA) and pairwise comparison after ANOVA analysis was performed using Fisher's Least Significant Difference *t*-test. Enumeration data were shown as rate or percentage and analyzed by Chi-square test. \* $p < 0.05$  indicates a significant difference.

## RESULTS

### Circ-ANXA7 expression is modulated in DDP-resistant NSCLC tissues and cells

circ-ANXA7 levels in resistant and non-resistant NSCLC tissues and normal tissues were tested by RT-qPCR. Compared with non-resistant NSCLC tissues and normal tissues, circ-ANXA7 was elevated in DDP-resistant NSCLC tissues, clarifying that circ-ANXA7 was associated with DDP resistance in NSCLC (Fig. 1A). Subsequently, analysis of the clinicopathological characteristics was implemented. Table 2 elucidated no difference in age, tumor size, gender, and metastasis between DDP-resistant patients with non-resistant patients. Nevertheless, DDP resistant patients had high levels of circ-ANXA7, deep invasion, low rate of tumor metastasis, and poor differentiation.

Likewise, in normal cells (HBE-1), NSCLC cell lines (A549 and H460) and DDP-resistant NSCLC cells (A549/DDP and H460/DDP), it was observed that circ-ANXA7 was the highest in DDP-resistant cells (Fig. 1B).

RNase R analysis and Act D analysis confirmed the annular characteristics of circ-ANXA7, showing that circ-ANXA7 was available to resist RNase R detachment, and its stability was better than linear ANXA7 mRNA (Fig. 1C–D). Additionally, circ-ANXA7 was primarily distributed in NSCLC cell cytoplasm (Fig. 1E). Kaplan-Meier analysis revealed that high circ-ANXA7 was associated with unpleasing overall survival in DDP-resistant NSCLC patients, as presented in Fig. 1F.

To sum up, circ-ANXA7 was stable and elevated in DDP-resistant NSCLC and might be implicated in NSCLC DDP resistance.

### Repressive circ-ANXA7 gene is available to suppress NSCLC's progression and strengthens DDP's sensitivity

It was found that A549 cells had stronger DDP resistance (Fig. 2A) than H460 cells, and circANXA7 expression in A549 and A549/DDP cells was higher than that in H460 and H460/DDP cells (Fig. 1B), so A549/DDP cells were selected for subsequent studies. As presented in Fig. 2B, circ-ANXA7 was repressed in A549/DDP cells after transfection with sh-circ-ANXA7. Silence of circ-ANXA7 declined DDP IC<sub>50</sub> (Fig. 2C). Cell proliferation and apoptosis were subsequently examined, and it was found that circ-ANXA7 gene knockout inhibited the viability of A549/DDP cells (Fig. 2D–E), while the apoptosis rate increased significantly (Fig. 2F). In addition, Transwell analysis confirmed that circ-ANXA7 silencing effectively blocked A549/DDP cell migration

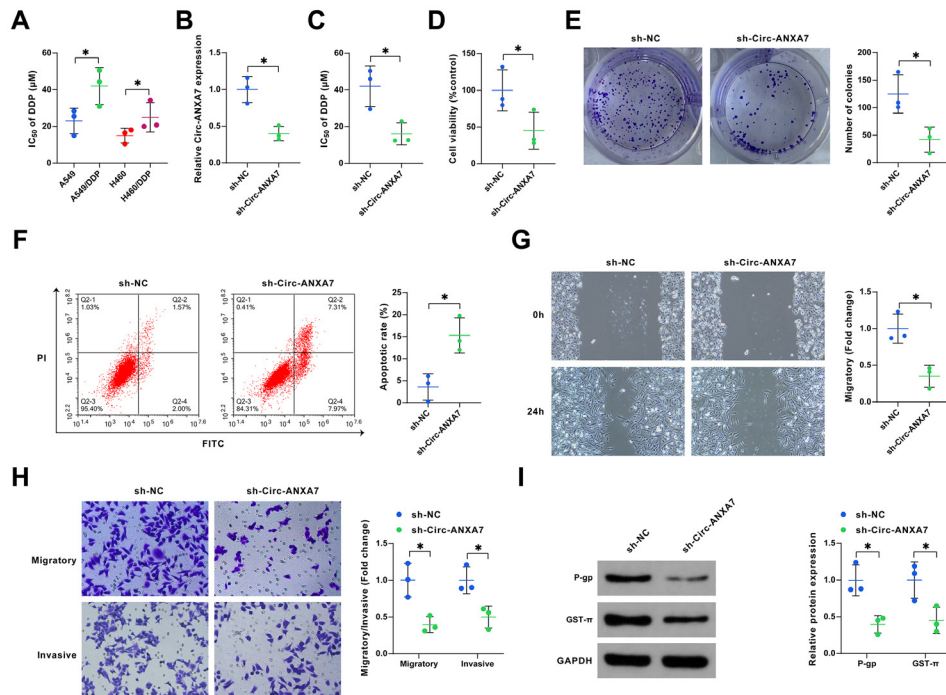


**Figure 2. Repression of circ-ANXA7 restrains NSCLC progression and strengthens DDP sensitivity**

(A) MTT analysis of IC<sub>50</sub>; (B) RT-qPCR test of sh-circ-ANXA7 transfection efficiency; (C) MTT analysis of IC<sub>50</sub> of DDP in A549/DDP cells after transfection; (D–E) MTT and colony formation assay detection of cell proliferative activity; (F) Flow cytometry test of cell apoptosis; (G–H) Transwell assay test of cell migration and invasion; (I) Western blot detection of drug-resistance associated proteins (P-GP and GST-π). Data were expressed as mean ± S.D. (Number of samples=3). \*P<0.05.

and invasion (Fig. 2G–H). Western blot analysis of drug resistance-associated proteins (P-gp and GST-π) was performed, elucidating that P-gp and GST-π in A549/DDP cells were lowered after suppressing circ-ANXA7, as presented in Fig. 2I.

In general, repressing circ-ANXA7 was available to suppress NSCLC progression and strengthened DDP sensitivity.

### Circ-ANXA7 performs as a sponge for miR-545-3p

To explore the novel mechanism of circ-ANXA7 to modulate NSCLC, prediction of the target miRNA of circ-ANXA7 was performed on the bioinformatics website starBase. circ-ANXA7 and miR-545-3p had complementary fragments (Fig. 3A). MiR-545-3p in A549/DDP cells was elevated after transfecting miR-545-3p mimic (Fig. 3B). The interaction of miR-545-3p with circ-ANXA7 was verified. As presented in Fig. 3C, elevated miR-545-3p constrained the luciferase activity of circ-ANXA7-WT 3'UTR, but it did not repress that of the mutant construct. Circ-ANXA7 and miR-545-3p were abundant in Ago2 antibody-immunoprecipitated RNA complex, but not in IgG antibody-immunoprecipitated RNA complex (Fig. 3D). Additionally, miR-545-3p expression was downregulated in DDP-resistant NSCLC tissues and cells (Fig. 3E–F), and clinical correlation analysis found that miR-545-3p was negatively associated with circ-ANXA7 in DDP-resistant NSCLC tissues (Fig. 3G).

All in all, miR-545-3p could be modulated by circ-ANXA7.

### Suppression of miR-545-3p turns around circ-ANXA7 knockdown's influence on NSCLC

To determine the functional regulation of circ-ANXA7 and miR-545-3p, sh-circ-ANXA7 and in-miR-

545-3p were constructed, and their efficacy was explicitly verified *in vitro*. It was discovered that silence of circ-ANXA7 elevated miR-545-3p (Fig. 4A). Subsequently, sh-circ-ANXA7 in combination with in-miR-545-3p or in-NC was transfected into A549/DDP cells. As presented in Fig. 4B, transfection with in-miR-545-3p declined miR-545-3p expression. MiR-545-3p expression was suppressed after sh-circ-ANXA7 was blocked by the miR-545-3p inhibitor. Additionally, it was observed that silence of circ-ANXA7 declined DDP IC<sub>50</sub>, but this effect was suppressed by in-miR-545-3p (Fig. 4C). In the meantime, inhibition of cell viability and promotion of apoptosis by circ-ANXA7 knockdown could be partially reversed by in-miR-545-3p (Fig. 4D–F). Additionally, the introduction of in-miR-545-3p was available to eliminate silenced circ-ANXA7's suppression of cell invasion and migration (Fig. 4G–H). Reduction in circ-ANXA7 led to a decrease in resistance-associated proteins, and this inhibition could be mitigated by supplementation with in-miR-545-3p (Fig. 4I).

In short, circ-ANXA7 modulated NSCLC cell progression and DDP sensitivity *via* absorbing miR-545-3p.

### MiR-545-3p immediately targets CCND1

As mentioned above, it was attempted to search for miR-545-3p's direct targets. As presented in Fig. 5A, starBase predicted the common binding site of miR-545-3p and CCND1. In the meantime, miR-545-3p mimic was available to weaken the luciferase activity of CCND1-WT 3'UTR, while no distinct change was presented in the luciferase activity of CCND1-MUT 3'UTR (Fig. 5B). Additionally, circ-ANXA7 and miR-545-3p were abundant in Ago2 antibody immunoprecipitation but not in IgG antibody immunoprecipitation (Fig. 5C). Compared with non-resistant and normal tissues, CCND1 in DDP-



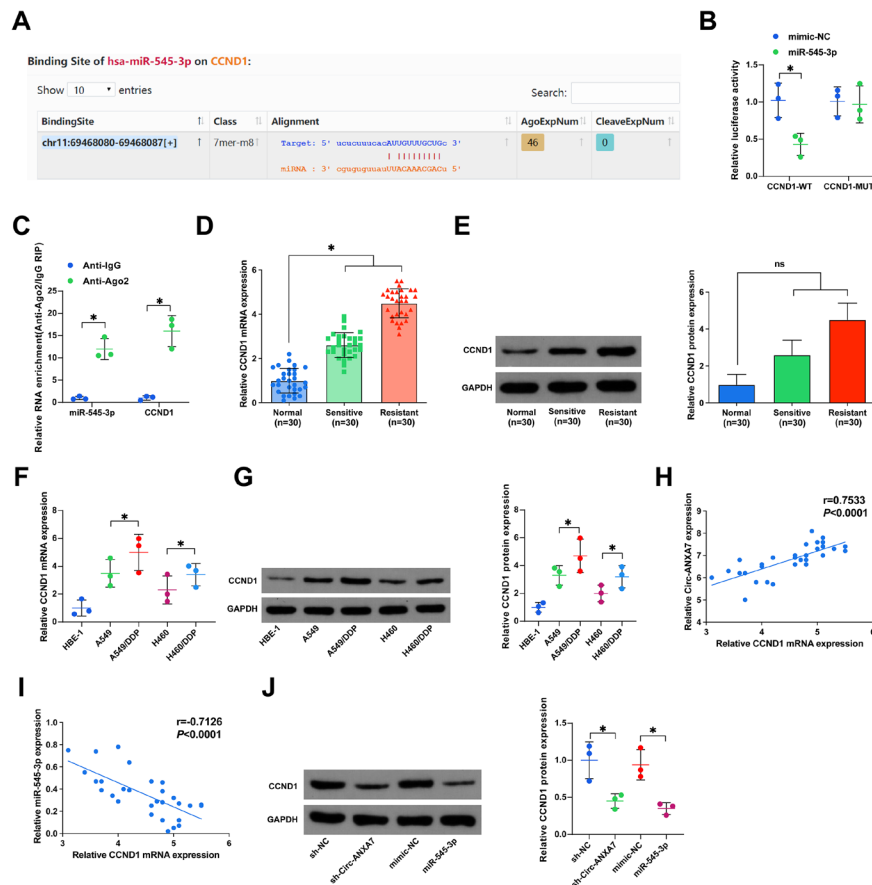


**Figure 5. CCND1 is the functional target of miR-545-3p**

(A) Bioinformatics sites forecast of binding sites of CCND1 with miR-545-3p; (B–C) Luciferase activity assay, and RIP assay evaluation of the interaction of CCND1 with miR-545-3p; (D–G) RT-qPCR and Western blot test of CCND1 in tissues and cells; (H–I) Pearson correlation analysis assessment of the association of CCND1 with miR-545-3p and circ-ANXA7. (J) Western blot examination of CCND1 after transfection with sh-circ-ANXA7 or miR-545-3p mimic. Data were expressed as mean  $\pm$  S.D. (Number of samples =3). \* $P$ <0.05..

resistant tissues was elevated (Fig. 5D–E). Likewise, CCND1 was also elevated in DDP-resistant NSCLC cells (Fig. 5F–G). In clinical tissues characterized by drug resistance, CCND1 was positively correlated with circ-ANXA7 expression and negatively correlated with miR-545-3p expression (Fig. 5H–I). In A549/DDP cells, downregulation of circ-ANXA7 or overexpression of miR-545-3p decreased CCND1 expression (Fig. 5J).

In brief, CCND1 was miR-545-3p's downstream gene.

### Circ-ANXA7 impacts NSCLC progression and DDP resistance via miR-545-3p/CCND1 axis

Functional tests were performed considering the association of miR-545-3p with circ-ANXA7 or CCND1. CCND1 overexpression plasmid strengthened CCND1 expression in A549/DDP cells (Fig. 6A–B). Then, to explain whether CCND1 mediates the effect of circ-ANXA7 on NSCLC progression and DDP resistance, A549/DDP cells were co-transfected with sh-circ-ANXA7 and CCND1 overexpression plasmid or empty plasmid. As presented in Fig. 6A–B, sh-circ-ANXA7 restrained CCND1 expression, which was reversed after co-transfection with the CCND1 overexpression plasmid. Additionally, the upregulation of CCND1 significantly restored the inhibitory effect of circ-ANXA7 silencing on DDP  $IC_{50}$  and cell viability in A549/DDP cells *in vitro* (Fig. 6C–E). In the meantime, downregulation of circ-ANXA7 promoted apoptosis, which was eliminated by

CCND1 overexpression plasmid (Fig. 6F). Additionally, elevating CCND1 restrained sh-circ-ANXA7-mediated repression of A549/DDP cell migration and invasion (Fig. 6G–H). Additionally, silenced circ-ANXA7-induced overexpression of P-gp and GST- $\pi$  was turned around by overexpressing CCND1 (Fig. 6I).

In short, circ-ANXA7 modulated NSCLC progression and DDP resistance via miR-545-3p/CCND1 axis.

### Loss of circ-ANXA7 reduces tumor growth *in vivo*

After sh-circ-ANXA7 or DDP treatment, tumor volume and weight were reduced, and sh-circ-ANXA7 and DDP treatment were provided with synergistic suppression (Fig. 7A–B). By examining circ-ANXA7 levels in xenografts, sh-Circ-ANXA7 did decrease circ-ANXA7 expression and promote miR-545-3p levels in excised tumors (Fig. 7C). Additionally, loss of circ-ANXA7 repressed CCND1 expression in excised tumors (Fig. 7D–E).

All in all, loss of circ-ANXA7 interacted with DDP therapy, thereby restraining tumor growth in xenograft tumor models.

### DISCUSSION

Globally, NSCLC is a deadly cancer with elevated morbidity and mortality (Cao *et al.*, 2021). DDP is the most frequently-adopted chemotherapy drug for the

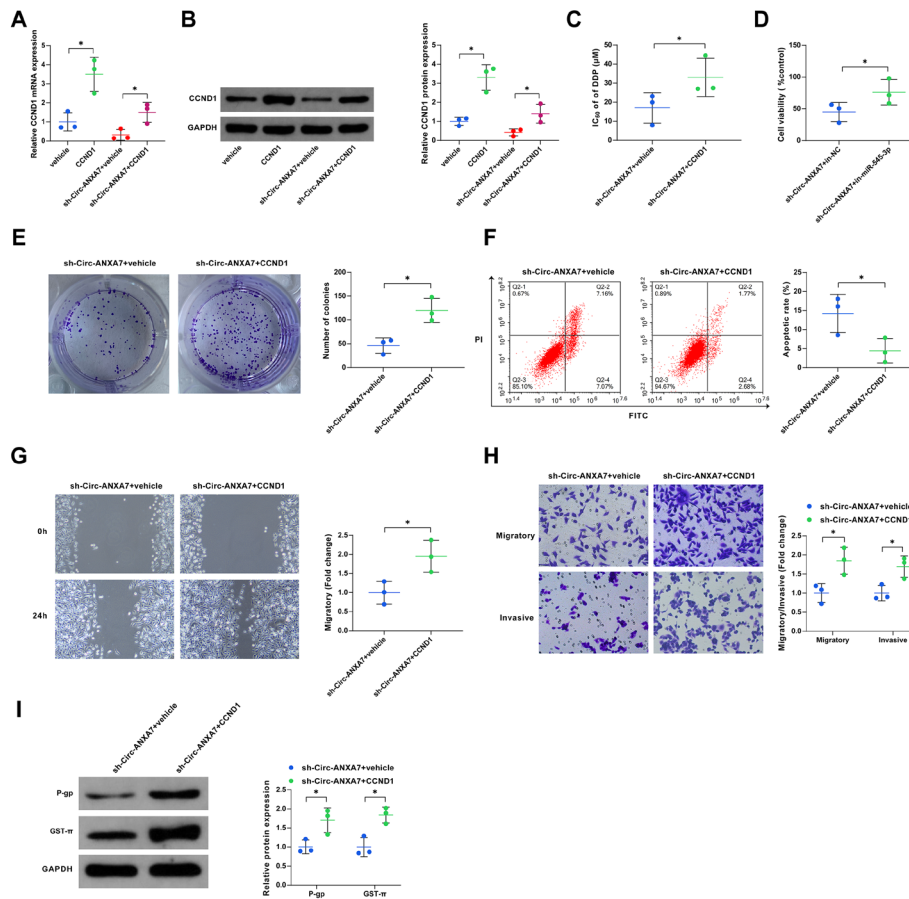


**Figure 6.** Circ-ANXA7 impacts NSCLC progression and DDP resistance via miR-545-3p/CCND1 axis

(A–B) RT-qPCR and Western blot examination of CCND1 in A549/DDP cells; (C) MTT analysis of IC<sub>50</sub> of DDP in A549/DDP cells; (D–E) MTT and colony formation assay detection of cell proliferative activity; (F) Flow cytometry test of cell apoptosis; (G–H) Transwell assay test of cell migration and invasion; (I) Western blot test of drug-resistance associated proteins (P-gp and GST-π). Data were expressed as mean ± S.D. (Number of samples = 3). \**P* < 0.05.

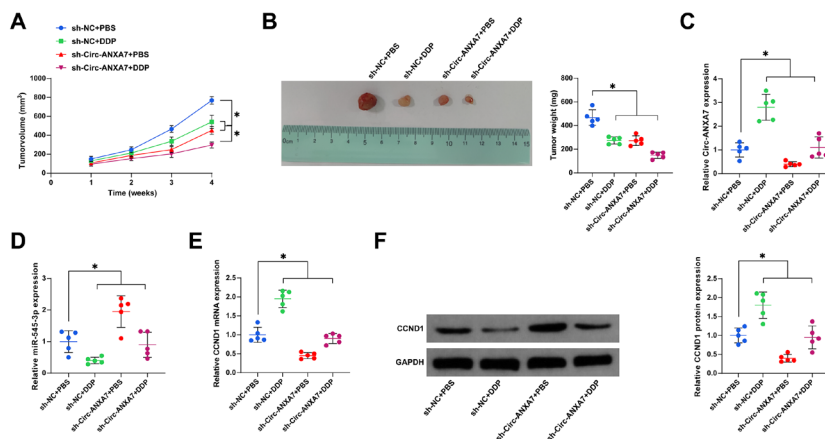


**Figure 7.** Loss of circ-ANXA7 lessens tumor growth in vivo

(A) Tumor volume changes of mice in each group; (B) Tumor weight of mice at 4th week; (C) Circ-ANXA7 and miR-545-3p in resected tumors; (D–E) CCND1 expression in resected tumors. Data were expressed as mean ± S.D. (Number of samples = 3). \**P* < 0.05.

treatment of NSCLC (Dong *et al.*, 2019). Nevertheless, DDP resistance severely limits its clinical efficacy (Hong *et al.*, 2020). Consequently, it was crucial to suppress DDP resistance for better treatment of NSCLC patients. It is reported that aberrant circRNA impacts NSCLC cancerization and chemotherapy resistance (Zhang *et al.*, 2021). In this study, it was first discovered that repres-

sion of circ-ANXA7 suppressed NSCLC progression and strengthened DDP sensitivity. Additionally, this study first verified the regulatory network of circ-ANXA7/miR-545-3p/CCND1.

Research has shown that the covalent closed structure of circRNAs makes them more stable in eukaryotes (Fu *et al.*, 2021). Likewise, the data displayed that circ-

ANXA7 after RNase R and Actinomycin D treatment was more stable than linear ANXA7. circRNAs exert critical roles in multiple biological processes of NSCLC (Liu *et al.*, 2021). For instance, in DDP-resistant NSCLC tissues and cells, circ\_PIP5K1A expression is augmented, while silencing circ\_PIP5K1A is available to restrain cancer progression and strengthen DDP sensitivity (Feng *et al.*, 2021). Additionally, silencing circ\_0076305 ameliorates the DDP sensitivity of NSCLC (Wang *et al.*, 2021). In other words, circRNAs modulate cancer progression and DDP resistance. This research focused on a novel circRNA (Circ-ANXA7) derived from host gene ANXA7 chr10 (75138745-75138766). Expression analysis displayed that circ-ANXA7 was elevated in DDP-resistant NSCLC tissues and cells, clarifying that circ-ANXA7 might participate in DDP resistance progression in NSCLC. As expected, it was discovered that circ-ANXA7 silencing inhibited the proliferative activity, migration, invasion, and DDP sensitivity of DDP resistant cells, but promoted apoptosis. Overall, the data have illustrated that circ-ANXA7 is a promoter of NSCLC progression and drug resistance. Nevertheless, circ-ANXA7 in patients' serum was not detected in this study. Notably, a recent report has clarified that exosomes-delivered hsa\_circ\_0014235 expedites DDP resistance and exacerbates NSCLC development *via* mediating miR-520a-5p/CDK4 pathway (Xu *et al.*, 2020). Consequently, it was a necessity to further examine circ-ANXA7 in NSCLC clinical serum samples in subsequent studies, which might offer novel data support for circ-ANXA7 as a promoter of NSCLC resistance.

As reported, the regulatory function of circRNA is associated with the miRNA/mRNA signaling network (Feng *et al.*, 2021). Notably, it is reported that circRNAs participate in various human cancers *via* effectively targeting miRNA to mediate gene (Liu *et al.*, 2022). For instance, silencing circ\_0007385 restrains malignant behavior and DDP resistance of NSCLC cells *via* miR-519d-3p/HMGB1 axis (Ye *et al.*, 2020). Circ\_0076305 modulates STAT3 and DDP resistance of NSCLC cells *via* absorbing miR-296-5p as a sponge (Dong *et al.*, 2019). Consequently, miR-545-3p was discovered to have a targeted binding site with circ-ANXA7. Foregoing studies have elucidated that miR-545-3p is silenced in NSCLC and performs as a tumor suppressor gene, restraining NSCLC progression and strengthening DDP sensitivity (Du *et al.*, 2021; Li, Liu, and Qin 2020). Likewise, in this study, it was discovered that miR-545-3p was silenced in DDP-resistant NSCLC tissues and cells and performed as a tumor suppressor gene. Additionally, it was first discovered that miR-545-3p was competitively adsorbed by circ-ANXA7, and upregulating miR-545-3p reversed the inhibitory effect of circ-ANXA7 loss on NSCLC progression and DDP resistance.

miRNAs are available to repress specific proteins after transcription *via* combining with the 3'UTR of target mRNA (Pang *et al.*, 2020). Consequently, the target genes of miR-545-3p were predicted, and CCND1 among numerous mRNAs has drawn our attention due to its relationship with DDP resistance (Zuo *et al.*, 2021). CCND1 performs as a carcinogen in NSCLC, promoting proliferation, migration, invasion, and drug resistance of NSCLC cells, and may become a potential therapeutic target for NSCLC (Huang *et al.*, 2020; Cui *et al.*, 2020; Liu *et al.*, 2020). Nevertheless, the mechanism of circ-ANXA7/miR-545-3p/CCND1 axis in NSCLC DDP resistance has not been explored. In this research, it was testified that elevated CCND1 was presented in DDP-resistant NSCLC tissues and cells. Additionally, it was

first discovered that miR-545-3p was implicated in DDP resistance in NSCLC *via* targeting CCND1.

In brief, circ-ANXA7 accelerated DDP resistance in NSCLC *via* the miR-545-3p/CCND1 axis, which might offer brand-new insights into the treatment of DDP resistance in NSCLC. Nevertheless, the potential involvement of downstream pathways was not considered in this study. In addition, future multicenter and animal studies are needed to further elucidate the role of circ-ANXA7 in DDP resistance in NSCLC.

## Declarations

**Data availability.** The figures and tables used to support the findings of this study are included in the article.

**Conflicts of interest.** The authors declare that they have no conflicts of interest.

**Acknowledgements.** The authors would like to show sincere thanks to those techniques who have contributed to this research.

## REFERENCES

- Cao F, Wu X, Shan Y, Zhang B, Wang H, Liu H, Yu H (2021) Circular RNA NEK6 contributes to the development of non-small-cell lung cancer by competitively binding with miR-382-5p to elevate BCAS2 expression at post-transcriptional level. *BMC Pulm Med* 21: 325. <https://doi.org/10.1186/s12890-021-01617-0>
- Cui D, Qian R, Li Y (2020) Circular RNA circ-CMPK1 contributes to cell proliferation of non-small cell lung cancer by elevating cyclin D1 *via* sponging miR-302e. *Mol Genet Genomic Med* 8: e999. <https://doi.org/10.1002/mgg3.999>
- Dong Y, Xu T, Zhong S, Wang B, Zhang H, Wang X, Wang P, Li G, Yang S (2019) Circ\_0076305 regulates cisplatin resistance of non-small cell lung cancer *via* positively modulating STAT3 by sponging miR-296-5p. *Life Sci* 239: 116984. <https://doi.org/10.1016/j.lfs.2019.116984>
- Du D, Cao X, Duan X, Zhang X (2021) Blocking circ\_0014130 suppressed drug resistance and malignant behaviors of docetaxel resistance-acquired NSCLC cells *via* regulating miR-545-3p-YAP1 axis. *Cytotechnology* 73: 571–584. <https://doi.org/10.1007/s10616-021-00478-z>
- Fan L, Li B, Li Z, Sun L (2021) Identification of autophagy related circRNA-miRNA-mRNA-subtypes network with radiotherapy responses and tumor immune microenvironment in non-small cell lung cancer. *Front Genet* 12: 730003. <https://doi.org/10.3389/fgene.2021.730003>
- Fan W, Chen L, Wu X, Zhang T (2021) Circ\_0031242 Silencing mitigates the progression and drug resistance in DDP-Resistant hepatoma cells by the miR-924/POU3F2 axis. *Cancer Manag Res* 13: 743–755. <https://doi.org/10.2147/cmar.S272851>
- Feng N, Guo Z, Wu X, Tian Y, Li Y, Geng Y, Yu Y (2021) Circ\_PIP5K1A regulates cisplatin resistance and malignant progression in non-small cell lung cancer cells and xenograft murine model *via* depending on miR-493-5p/ROCK1 axis. *Respir Res* 22: 248. <https://doi.org/10.1186/s12931-021-01840-7>
- Fu B, Liu W, Zhu C, Li P, Wang L, Pan L, Li K, Cai P, Meng M, Wang Y, Zhang A, Tang W, An M (2021) Circular RNA circ-CBM1 promotes breast cancer brain metastasis by modulating miR-125a/BRD4 axis. *Int J Biol Sci* 17: 3104–3117. <https://doi.org/10.7150/ijbs.58916>
- Guo X, Wang H, Jiang H, Qiao L, Wang X (2022) Circ\_0011292 Enhances paclitaxel resistance in non-small cell lung cancer by regulating miR-379-5p/TRIM65 axis. *Cancer Biother Radiopharm* 37: 84–95. <https://doi.org/10.1089/cbr.2019.3546>
- Hong W, Xue M, Jiang J, Zhang Y, Gao X (2020) Circular RNA circ-CPA4/let-7 miRNA/PD-L1 axis regulates cell growth, stemness, drug resistance and immune evasion in non-small cell lung cancer (NSCLC). *J Exp Clin Cancer Res* 39: 149. <https://doi.org/10.1186/s13046-020-01648-1>
- Hu X, Wang P, Qu C, Zhang H, Li L (2021) Circular RNA Circ\_0000677 promotes cell proliferation by regulating microRNA-106b-5p/CCND1 in non-small cell lung cancer. *Bioengineered* 12: 6229–6239. <https://doi.org/10.1080/21655979.2021.1965697>
- Huang SR, Jin SS, Xu B, Wang RP (2020) Puerarin alleviates the progression of non-small cell lung cancer by regulating the miR-342/CCND1 axis. *Neoplasma* 67: 1244–1255. [https://doi.org/10.4149/neo\\_2020\\_191107N1145](https://doi.org/10.4149/neo_2020_191107N1145)
- Ju ZS, Sun B, Bao D, Zhang XF (2020) Effect of lncRNA-BLACAT1 on drug resistance of non-small cell lung cancer cells in DDP chem-

- otherapy by regulating cyclin D1 expression. *Eur Rev Med Pharmacol Sci* **24**: 9465–9472. [https://doi.org/10.26355/eurrev\\_202009\\_23031](https://doi.org/10.26355/eurrev_202009_23031)
- Li H, Liu F, Qin W (2020) Circ\_0072083 interference enhances growth-inhibiting effects of cisplatin in non-small-cell lung cancer cells via miR-545-3p/CBLL1 axis. *Cancer Cell Int* **20**: 78. <https://doi.org/10.1186/s12935-020-1162-x>
- Liu B, Chen D, Chen S, Saber A, Haisma H (2020) Transcriptional activation of cyclin D1 via HER2/HER3 contributes to EGFR-TKI resistance in lung cancer. *Biochem Pharmacol* **178**: 114095. <https://doi.org/10.1016/j.bcp.2020.114095>
- Liu D, Li W, Zhong F, Yin J, Zhou W, Li S, Sun X, Xu J, Li G, Wen Y, Wang J, Hong J, Cheng Z, Yuan J, Dai L, Sun J, Wang J, Qiu C, Wang G, Zou C (2020) METTL7B Is required for cancer cell proliferation and tumorigenesis in non-small cell lung cancer. *Front Pharmacol* **11**: 178. <https://doi.org/10.3389/fphar.2020.00178>
- Liu Y, Li C, Liu H, Wang J (2021) Circ\_0001821 knockdown suppresses growth, metastasis, and TAX resistance of non-small-cell lung cancer cells by regulating the miR-526b-5p/GRK5 axis. *Pharmacol Res Perspect* **9**: e00812. <https://doi.org/10.1002/prp2.812>
- Liu Y, Zhai R, Hu S, Liu J (2022) Circular RNA circ-RNF121 contributes to cisplatin (DDP) resistance of non-small-cell lung cancer cells by regulating the miR-646/SOX4 axis. *Anticancer Drugs* **33**: e186–e197. <https://doi.org/10.1097/cad.0000000000001184>
- Meng Y, Yang L, Wei X, Luo H, Hu Y, Tao X, He J, Zheng X, Xu Q, Luo K, Yu G, Luo Q (2021) CCT5 interacts with cyclin D1 promoting lung adenocarcinoma cell migration and invasion. *Biochem Biophys Res Commun* **567**: 222–229. <https://doi.org/10.1016/j.bbrc.2021.04.105>
- Pang J, Ye L, Zhao D, Zhao D, Chen Q (2020) Circular RNA PRMT5 confers cisplatin-resistance via miR-4458/REV3L axis in non-small-cell lung cancer. *Cell Biol Int* **44**: 2416–2426. <https://doi.org/10.1002/cbin.11449>
- Shao N, Song L, Sun X (2021) Exosomal circ\_PIP5K1A regulates the progression of non-small cell lung cancer and cisplatin sensitivity by miR-101/ABCC1 axis. *Mol Cell Biochem* **476**: 2253–2267. <https://doi.org/10.1007/s11010-021-04083-8>
- Song HM, Meng D, Wang JP, Zhang XY (2021) circRNA hsa\_circ\_0005909 predicts poor prognosis and promotes the growth, metastasis, and drug resistance of non-small-cell lung cancer via the miRNA-338-3p/SOX4 pathway. *Dis Markers* **2021**: 8388512. <https://doi.org/10.1155/2021/8388512>
- Wang X, Wang H, Jiang H, Qiao L, Guo C (2021) Circular RNA circ\_0076305 Promotes Cisplatin (DDP) Resistance of non-small cell lung cancer cells by regulating ABCC1 through miR-186-5p. *Cancer Biother Radiopharm* <https://doi.org/10.1089/cbr.2020.4153>
- Wang Y (2021) circ-ANXA7 facilitates lung adenocarcinoma progression via miR-331/LAD1 axis. *Cancer Cell Int* **21**: 85. <https://doi.org/10.1186/s12935-021-01791-5>
- Wei D, Sun L, Feng W (2021) hsa\_circ\_0058357 acts as a ceRNA to promote non-small cell lung cancer progression via the hsa-miR-24-3p/AVL9 axis. *Mol Med Rep* **23**. <https://doi.org/10.3892/mmr.2021.12109>
- Wu Z, Gong Q, Yu Y, Zhu J, Li W (2020) Knockdown of circ-ABC10 promotes sensitivity of lung cancer cells to cisplatin via miR-556-3p/AK4 axis. *BMC Pulm Med* **20**: 10. <https://doi.org/10.1186/s12890-019-1035-z>
- Xu J, Ni L, Zhao F, Dai X, Tao J, Pan J, Shi A, Shen Z, Su C, Zhang Y (2021) Overexpression of hsa\_circ\_0002874 promotes resistance of non-small cell lung cancer to paclitaxel by modulating miR-1273f/MDM2/p53 pathway. *Aging (Albany NY)* **13**: 5986–6009. <https://doi.org/10.18632/aging.202521>
- Xu X, Tao R, Sun L, Ji X (2020) Exosome-transferred hsa\_circ\_0014235 promotes DDP chemoresistance and deteriorates the development of non-small cell lung cancer by mediating the miR-520a-5p/CDK4 pathway. *Cancer Cell Int* **20**: 552. <https://doi.org/10.1186/s12935-020-01642-9>
- Ye Y, Zhao L, Li Q, Xi C, Li Y, Li Z (2020) circ\_0007385 served as competing endogenous RNA for miR-519d-3p to suppress malignant behaviors and cisplatin resistance of non-small cell lung cancer cells. *Thorac Cancer* **11**: 2196–2208. <https://doi.org/10.1111/1759-7714.13527>
- Zhang W, Song C, Ren X (2021) Circ\_0003998 Regulates the progression and docetaxel sensitivity of DTX-resistant non-small cell lung cancer cells by the miR-136-5p/CORO1C axis. *Technol Cancer Res Treat* **20**: 1533033821990040. <https://doi.org/10.1177/1533033821990040>
- Zhang Y, Ge P, Zhou D, Xing R, Bai L (2021) Circular RNA FOXO3 accelerates glycolysis and improves cisplatin sensitivity in lung cancer cells via the miR-543/Foxo3 axis. *Oncol Lett* **22**: 839. <https://doi.org/10.3892/ol.2021.13100>
- Zhang Y, Zeng S, Wang T (2021) Circular RNA hsa\_circ\_0002360 promotes non-small cell lung cancer progression through upregulating matrix metalloproteinase 16 and sponging multiple micorRNAs. *Bioengineered* **12**: 12767–12777. <https://doi.org/10.1080/21655979.2021.1999370>
- Zhu K, Zhu J, Geng J, Zhang Y, Qin Y, Wang F, Weng Y (2021) circSNX6 (hsa\_circ\_0031608) enhances drug resistance of non-small cell lung cancer (NSCLC) via miR-137. *Biochem Biophys Res Commun* **567**: 79–85. <https://doi.org/10.1016/j.bbrc.2021.06.032>
- Zuo Y, Zheng W, Tang Q, Liu J, Wang S, Xin C (2021) miR-576-3p overexpression enhances cisplatin sensitivity of ovarian cancer cells by dysregulating PD-L1 and cyclin D1. *Mol Med Rep* **23**. <https://doi.org/10.3892/mmr.2020.11719>